View Article Online
View Journal

NJC

Accepted Manuscript

This article can be cited before page numbers have been issued, to do this please use: J. Dinda, A. Nandy, T. Samanta, P. Mitra, K. Das Saha, S. S. Al-deyab, S. K. Seth and S. Mallick, *New J. Chem.*, 2016, DOI: 10.1039/C5NJ02979A.

This is an *Accepted Manuscript*, which has been through the Royal Society of Chemistry peer review process and has been accepted for publication.

Accepted Manuscripts are published online shortly after acceptance, before technical editing, formatting and proof reading. Using this free service, authors can make their results available to the community, in citable form, before we publish the edited article. We will replace this *Accepted Manuscript* with the edited and formatted *Advance Article* as soon as it is available.

You can find more information about *Accepted Manuscripts* in the Information for Authors.

Please note that technical editing may introduce minor changes to the text and/or graphics, which may alter content. The journal's standard Terms & Conditions and the Ethical guidelines still apply. In no event shall the Royal Society of Chemistry be held responsible for any errors or omissions in this *Accepted Manuscript* or any consequences arising from the use of any information it contains.

ROYAL SOCIETY OF CHEMISTRY

www.rsc.org/njc

View Article Online
DOI: 10.1039/C5NJ02979A

Journal Name

ARTICLE

Synthesis of Gold(III)←Gold(I)-NHC Through Disproportionation: Role of Gold(I)-NHC in the induction of apoptosis in HepG2 cells

Received 00th January 20xx,
Accepted 00th January 20xx

DOI: 10.1039/x0xx00000x

www.rsc.org/

Abhishek Nandy [a], Tapastaru Samanta, [b] Sumana Mallick, [a] Partha Mitra, [c] Saikat Kumar Seth, [d] Krishna Das Saha [a*], Salem S. Al-Deyab [e] and Joydev Dinda [f*]

Starting from the proligand 2-[(6-methylpyridin-2-yl)]imidazo[1,5-a]pyridin-4-ylium hexafluorophosphate (**1**.PF_6), three new complexes, viz. $[Au(1)_2]$ $[PF_6]$ (2), $[1/2AuCl_2$, $1/2AuCl_4]$– $[(1H)]^+$ (**3**), and $[Au(1)Cl_3]$ (**4**) have been synthesized and characterized employing different spectroscopic methods. $[Au(1)Cl_3]$ (**4**) has been synthesized by disproportionation process. During transformation of **2** to **4**, the annelated proligand stabilizes both Au(I) and Au(III), the isolation of the intermediate (**3**) confirming the conversion of Au(I)→Au(III) through disproportionation pathway. The solid state structures of **2**, **3** and **4** have been determined. Linear geometry was observed in **2** whereas complex **4** adopted square-planar geometry. The gold complexes **2** and **4** have been subjected to growth inhibitory studies. Complex **2** induced apoptosis in HepG2 cells along with increased expressions of proteins involved in the mitochondrial death pathway, suggesting that apoptosis may occur via the mitochondrial death pathway.

Introduction

Metals are essential cellular components of living organisms selected by nature to function in several indispensable biochemical processes. Nowadays, compounds of noble metals with wide structural diversity are being used as therapeutic agents for cancer treatment. [1] The discovery of the antitumour properties of cisplatin by Rosenberg [2] energized the field of metal based drugs and created room for other metals especially gold for developing therapeutic agents against tuberculosis, cancer and other infectious diseases. [3-5]

One of the main disadvantages of d^{10} metal complexes as drug is the quick release of metal, which deactivates the drug due to easy disruption of metal-ligand bond (weak metal-ligand bond). [6] This problem may be overcome by introducing the N-heterocyclic carbene as 'spectator' ligands, [7] which form stronger metal-carbene bonds than others. For this reason electron-rich NHCs, that often form strong bonds with a broad spectrum of metal to produce stable complexes in different oxidation states, are considered as versatile ligands in organometallic chemistry. [8] Possibly the first reports on biological activity of metal-NHC complexes were published in 1996 by Cetinkaya et al., who described the antibacterial properties of ruthenium(II)-NHC complexes. [9] Afterwards, the number of literature reports on metal-NHC complexes in biomedical sciences kept rising. Presently, research on the biological potential of metal-NHC complexes is one of the most active areas within the emerging field of bio-inorganic chemistry. [10] In particular the development of metal based drugs for the treatment of cancer or infectious diseases has been in the forefront of state-of-the art research on biological screening and drug evaluation of metal-NHC complexes. [11] Yet, to date only a limited number of Au(I) and Au(III)-NHCs have been used as anticancer agents among novel non-platinum based antitumor agents. [12] But gold complexes have recently gained promising attention because of their strong anti-proliferative effects against several panels of cancer cell lines. [11,12] Berners-Price, Barnard, Filipovska and others developed mitochondria targeted antitumor agents using Au(I)-N-heterocyclic carbene, where selective mitochondria targeting and selective thioredoxin reductase inhibition properties were achieved using a single molecular species. [4, 13, 14]

Although the biological applications of gold(I) and gold(III) complexes are wide, relatively few Au(III) complexes are reported, though Au(III) may be considered as alternative to Pt(II). Since Au(III) is isoelectronic with Pt(II) and both metals are expected to form complexes with square planar geometries, one may expect Au(III) complexes to display biological properties similar to those of cisplatin. [15] So far most of the literature reports synthesis of Au(III)–NHC *via*

Published on 05 May 2016. Downloaded by Université Laval on 09/05/2016 06:34:27.

New Journal of Chemistry Accepted Manuscript

Please do not adjust margins

View Article Online
DOI: 10.1039/C5NJ00970A

Published on 05 May 2016. Downloaded by Université Laval on 09/05/2016 06:34:27.

treatment of the corresponding Au(I) complex with Cl_2, Br_2, or I_2. Other processes like direct synthesis of Au(III)-NHC that utilizes an Au(III) precursor (e.g., $KAuCl_4$) or the use of $PhCl_2I$ for Au(I) → Au(III)-NHC transformation is also reported. We recently developed and applied a disproportionation scheme for the same purpose that avoided the need for Cl_2, Br_2 or other noxious agents. [16] This protocol has been used on a series of ligands, and is expected to become common in practice.

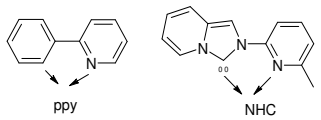

Chart 1. C, N donor ligands

Recently, the C, N donor 2-phenylpyridine ligand has also come into limelight due to biochemical application. Au complexes of 2-phenylpyridine have shown cytotoxicity towards MOLT-4 and other cancer cell lines. [17] Chemical and biological properties of Pt, Rh, Ir and other complexes [18] of 2-phenylpyridine ligand have drawn attention of the investigators. Encouraged by these results, we also designed a similar C, N donor NHC ligand, viz. 2-(6-methyl-pyridin-2-yl)-2*H*-imidazo[1,5-*a*]pyridin-4-ylium salt (shown in Chart 1). The reason for its preference as NHC are: (i) it forms highly stable complexes in presence of air and moisture, (ii) it stabilizes complexes in various oxidation states, (iii) it is not selective, forming complexes with most of the metals in the periodic table and (iv) it contains the imidazole ring, which is a biologically ubiquitous ligand. With this background, we have studied its gold complexes as anti-cancer agents. The possible anticancer activity of Au-NHCs attracted our attention due to our continued interest in novel organometallic anticancer drugs.[16] The present manuscript describes our findings on their synthesis and the anticancer properties.

Results and Discussion

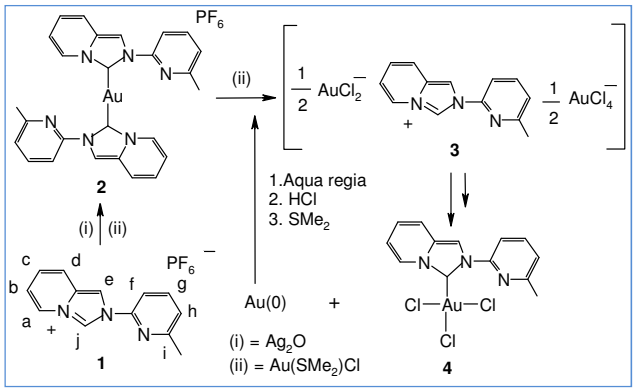

Scheme1. Synthesis of Au(I) and Au(III) complexes *via* disproportionation. The letters surrounding the structure of **1** refer to the NMR assignments; see the Experimental section.

Synthetic strategy of 1•HPF_6, 2, 3 and 4

The imidazolium salt 2-[(6-methylpyridin-2-yl)]imidazo [1,5-a]pyridine-4 ium hexaflurophosphate, **1**•HPF_6, has been synthesized via formylative cyclization reaction of the corresponding Schiff base 2-(6-methylpyridyl)-N-(2-pyridyl)methylamine using reported conditions. [19] Imidazolium salts are common precursors to NHC ligands; transfer of imidazolium salt derived proligands to group d[10] metal complexes has been conveniently achieved via silver (I) complexes. [20] [Au(**1**)$_2$(PF_6)] (**2**) was obtained via silver-carbene transfer method using [Au(Me_2S)Cl] as illustrated in Scheme 1. When (**2**) was stirred for 4 h with excess [Au(Me_2S)Cl] in CH_3CN, a light yellow solution was obtained along with the precipitation of Au(0); after filtration and removal of the solvent the product was characterized as [1/2$AuCl_2$, 1/2$AuCl_4$]$^-$ [(1H)]$^+$ (**3**). When we continued stirring the same mixture for more than 6 h, an orange-red solution was formed with slight yellow precipitation. After removal of the solvents and washing with ethanol-water (1:2), the dried solid mass was identified as **4**. The spectral characterizations support the formation of NHC-$AuCl_3$ (**4**). Interestingly, without use of noxious Cl_2(g), the gold(III) complex [Au(**1**)Cl_3] (**4**) was prepared by novel disproportionation pathway using excess Au(SMe_2)Cl with **2** as shown in scheme 1, an established procedure developed in our lab and applicable to other systems also.[12,15,17,20] The metallic gold produced in this method could be recycled to synthesize [Au(Me_2S)Cl]. Additionally, isolation of the intermediate **3** supports the development of the reaction through disproportionation which is shown in scheme 2.

Characterization of 1-4

Formation of the proligand **1** was confirmed by ^{1}H and ^{13}C NMR as reported earlier. [19] The complexes **2**, **3** and **4** were studied by elemental analysis, ^{1}H and ^{13}C NMR spectroscopy, and the results are consistent with their proposed formulations. The disappearance of the imidazolium NC*H*N proton signal around 10.8 ppm in ^{1}H NMR spectrum and the downfield shift of α-pyridyl proton peak ('a') confirm the formation of **2**. In ^{13}CNMR spectrum, the carbenic carbon peak appears at 171.9 ppm for **2** [at 152.6 ppm in proligand **1**.HPF_6]. The ^{1}H and ^{13}C NMR spectra of **3** were almost similar to those of **1**.HPF_6. Only 0.33 ppm down field shift was observed for the imidazolium C2-H proton, may be due to the presence of [$AuCl_4$]$^-$ which may form a H-bond with it. The conclusion was supported by solid state structure determination. The pattern of ^{1}H NMR spectrum of **4** was similar to that of **2** but some downfield shift of aromatic protons was observed. The carbenic signal of **4** appears at 159.3 ppm, upfield shifted from that in **2**, may be due to coordination with gold(III), a known phenomenon. [21, 22]

New Journal of Chemistry Accepted Manuscript

This journal is © The Royal Society of Chemistry 20xx

Please do not adjust margins

View Article Online
DOI: 10.1039/C5NJ00790A

Table 1 Crystallographic data and structure refinement parameters for complexes **2**, **3** and **4.**

	2	**3**	**4**
Empirical formula	$C_{28}H_{25}AuF_6N_7P$	$C_{13}H_{12}N_3Cl_3Au$	$C_{13}H_{11}AuCl_3$
Formula weight	801.49	513.57	512.56
Temperature (K)	150(2)	293(2)	293(2)
Wavelength (Å)	0.71073	0.71073	0.71073
Crystal system	Monoclinic	Triclinic	Triclinic
Unit cell dimensions			
a (Å)	7.6118(10)	4.3231(16)	7.8357(9)
b (Å)	19.781(3)	9.305(4)	9.7387(11)
c (Å)	18.635(2)	19.116(7)	11.0588(12)
α (º)	90	87.056(10)	115.506(2)
β(º)	90.601(3)	86.072(10)	92.671(2)
γ(º)	90	79.910(10)	96.763(2)
Volume, $Å^3$	2805.8(6)	754.7(5)	751.88(15)
Z	4	2	2
Calcd. density ($Mg/m^{3)}$	1.897	2.260	2.264
Absorption coefficient (mm^{-1})	5.374	10.269	10.307
F(000)	1560	482	480
Crystal size (mm)	0.21 × 0.17 × 0.14	0.19 × 0.12 × 0.07	0.19 x 0.13 x 0.06
θ range (˚)	1.50 -29.29	1.7-31.99	2.05 -29.35
Limiting indices	-10<=h<=9, -25<=k<=26, -24<=l<=25	-6<=h<=6, -13<=k<=13, -27<=l<=26	-10<=h<=10, -12<=k<=13, -14<=l<=14
Reflections collected / unique data / R(int)	32002 /7305 / 0.0546	11721 / 4405/ 0.0267	8614 / 3658 / 0.0295
Observed data / parameters	4818 / 391	2936 / 185	3179/182
Goodness-of-fit on F^2	1.057	0.997	1.038
Final R indices [I>2σ(I)]	R1 = 0.0394, wR2 = 0.0788	R1 = 0.0280, wR2 = 0.0602	R1 = 0.0269, wR2 = 0.0487
R indices (all data)	R1 = 0.0734, wR2 = 0.0899	R1 = 0.0527, wR2 = 0.0679	R1 = 0.0345, wR2 = 0.0508

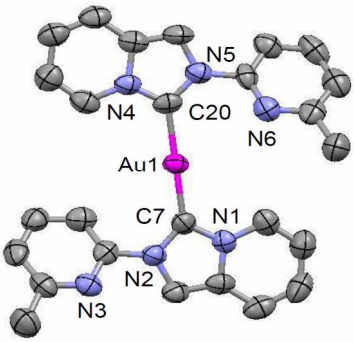

Fig. 1. ORTEP view of single crystal X-ray structure of **2** with 50% probability (H atom, CH_3CN and anion PF_6 have been removed for clarity). Selected bond lengths (Å) and angles (°): Au(1)-C(7) 2.008(5), Au(1)-C(20) 2.023(5), N(1)-C(7) 1.357(7), N(2)-C(7) 1.365(7), N(4)-C(20) 1.349(7), N(5)-C(20) 1.354(7), C(7)-Au(1)-C(20) 179.1(2), N(1)-C(7)-N(2) 102.7(4), N(4)-C(20)-N(5) 104.5(4).

X-ray crystal structure description of [Au(1)$_2$ (PF$_6$)] complex (2): [Au(**1**)$_2$(PF$_6$)] (**2**) was synthesized by the silver-carbene transmetallation method. Single crystals suitable for X-ray diffraction were grown by slow diffusion of diethyl ether into a saturated acetonitrile solution of the complex. The ORTEP view of **2** is shown in Fig. 1. Crystallographic parameters are listed in Table 1. The selected bond parameters are listed in figure caption and crystallographic parameters are listed in Table 1. The molecule crystallized with monoclinic symmetry with P21/n space group. In the mononuclear unit, the linear bis-carbene gold(I) complex possesses dissimilar Au(I)-$C_{carbene}$ bond lengths: Au(1)-C(7) = 2.008(5) and Au(1)-C(20) = 2.020(4) Å. The Au(I)-C bond distances are comparable with other known Au(I)-NHC bicoordinated linkages [16a,21] and within the sum of van der Waals radii of gold and carbon atoms [Au-C = 2.108 Å]. The C(7)-Au(1)-C(20) bond connectivity is almost linear, with dihedral angle of 179.26(18)°. In complex **2**, the bond parameters are very similar to other Au(I)-NHC annelated systems [21] developed by our group as mentioned in Table 2.

X-ray structure description of [Au(1)Cl$_3$] complex (3)

The single crystals of **3** suitable for X-ray diffraction were grown by slow diffusion of diethyl ether into saturated acetonitrile solution of the complex. The colorless complex **3** crystallizes in the 'P21/c' space group. The ORTEP view of **3** is shown in Fig. 2. The selected bond parameters are listed in figure caption and probable mechanism of formation is shown Scheme 2. The N(1)-C(7) and N(2)-C(7) separations are 1.351(5) and 1.330(5) Å and N(1)-C(7)-N(2) angle is 108.3(3)°, consistent with values for other imidazolium salts. [23] The imidazolium proton H(7) forms shortest H--bonding, C(7)-H(7)---Cl(2) = 2.803 Å and largest C(7)-H(7)-Cl(2) angle, 161.43° (shown in Scheme 3). Presumably the removal of HCl leads to formation of NHC-AuCl$_3$ complex, providing support to the mechanistic scheme depicted in scheme 2

Published on 05 May 2016. Downloaded by Université Laval on 09/05/2016 06:34:27.

New Journal of Chemistry Accepted Manuscript

Please do not adjust margins

View Article Online
DOI: 10.1039/C5NJ02979A

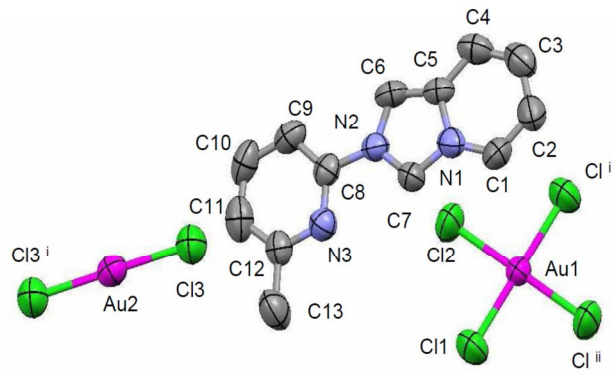

Fig. 2. ORTEP view (50% probability) of single crystal X-ray structure of **3** (H atoms have been removed for clarity). Symmetry transformations used to generate equivalent atoms: *: (-x+2, -y+1, -z+1) and #: (-x, -y+2, -z). Selected bond lengths (Å) and angles (°) of **3** are: Au(1)-Cl(1) 2.2713(12), Au(1)-Cl(1)#1 2.2713(12), Au(1)-Cl(2) 2.2734(14), Au(1)-Cl(2)#1 2.2734(14), Au(2)-Cl(3) 2.2622(13), Au(2)-Cl(3)#2 2.2622(13), N(1)-C(7) 1.351(5), N(2)-C(7) 1.330(5), Cl(1)#1-Au(1)-Cl(1) 180.00(6), Cl(1)#1-Au(1)-Cl(2) 90.08(4), Cl(1)-Au(1)-Cl(2) 89.92(4), Cl(1)#1-Au(1)-Cl(2)#1 89.90(5), Cl(1)-Au(1)-Cl(2)#1 90.10(5), Cl(2)-Au(1)-Cl(2)#1 180.000(1), Cl(3)-Au(2)-Cl(3)#2 180.0, N(1)-C(7)-N(2) 108.1(4).

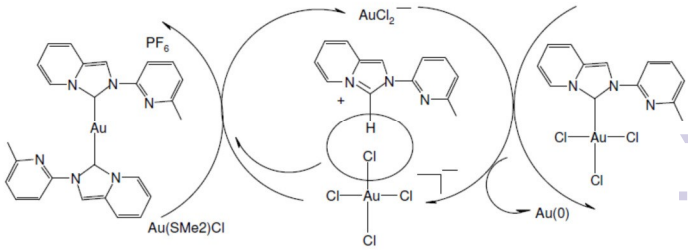

Scheme 2. Probable mechanism of Au(I)→Au(III) transformation *via* disproportion.

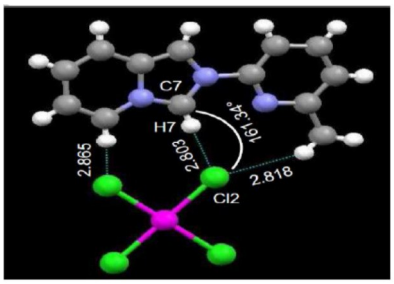

Scheme 3. C(7)-H(7)---Cl(2) H--bonding in support of mechanism in scheme 2.

Table 2. Comparative bond parameters of Au(I) and Au(III)–N-heterocyclic carbene complexes of annelated systems

	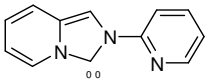	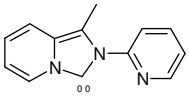	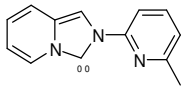
Ref.	21a	21b	present work
$[Au(NHC)_2]^{1+}$			
Au(I)-$C_{carbene}$ (Å)	----------	Au(1)–C(1) = 2.008(5)	Au(1)-C(7) = 2.008(5)
	----------	Au(1)–C(14) = 2.018(5)	Au(1)-C(20) =2.020(4)
N(1)-Au(1)-N(2)	----------	N(1)-C(1)–N(2) = 104.1(5)	N(1)-C(7)-N(2)=102.8(4)
		N(4)-C(14)-C(5)= 103.5(5)	N(4)-C(20)-N(5) =104.3(4)
$[Au(NHC)Cl_3]$#			
Au(I)-$C_{carbene}$ (Å)	Au(1)–C(7) = 2.005(9)	Au(1)–C(1) = 1.996(6)	Au(1)-C(7) = 1.995(4)
		Au(1)–C(14) = 2.014(5)	
Au(1)-Cl	Au(1)–Cl(1) = 2.301(3)	Au(1)–Cl(1) = 2.2984(16) Au(1)–Cl(2)= 2.3150(16)	Au(1)-Cl(1) =2.3063(12) Au(1)-Cl(2) =2.2893(12) Au(1)-Cl(3) = 2.2824(12)
	Au(1)–Cl(2)=2.289(3) Au(1)–Cl(3) = 2.292(3)	----------	
N(1)-Au(1)-N(2)	N(1)-C(7)-N(2)= 106.8(8)	N(1)-C(1)-N(2) = 105.3(5) N(4)-C(14)-N(5) = 106.2(4)	N(1)-C(7)-N(2) =106.3(3)

in case of Ref [21b] $[Au(NHC)_2Cl_2]PF_6$

Published on 05 May 2016. Downloaded by Université Laval on 09/05/2016 06:34:27.

New Journal of Chemistry Accepted Manuscript

This journal is © The Royal Society of Chemistry 20xx

Please do not adjust margins

View Article Online
DOI: 10.1039/C5NJ02979A

Journal Name

ARTICLE

Published on 05 May 2016. Downloaded by Université Laval on 09/05/2016 06:34:27.

New Journal of Chemistry Accepted Manuscript

X-ray structure description of [Au(1)Cl_3] complex (4)

The solid state structure of **4** was confirmed by X-ray diffraction studies. The ORTEP view of **4** is shown in Fig. 3. The orange-red complex crystallizes in the 'P21/c' space group. It has a four-coordinate gold atom in a square-planar environment, as expected for d^8 metals. The Au(III)CCl_3 coordination sphere forms a planar unit (maximum deviations less than 0.02 Å) where appending $N_{pyridine}$ remains uncoordinated with Au(III).

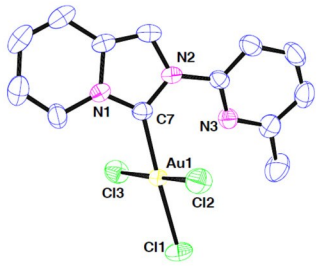

Fig. 3. ORTEP view (50% probability) of single crystal X-ray structure of **4** (H atoms have been removed for clarity). Selected bond lengths (Å) and angles (°) are: Au(1)-C(7) 1.996(4), Au(1)-Cl(1) 2.3062(12), Au(1)-Cl(2) 2.2895(12), Au(1)-Cl(3) 2.2826(12), Au(I)---N(3) 2.812, N(1)-C(7) 1.399(5), N(2)-C(7) 1.347(5), C(7)-Au(1)-Cl(1) 176.34(12), C(7)-Au(1)-Cl(2) 89.32(11), C(7)-Au(1)-Cl(3) 87.41(11), Cl(1)-Au(1)-Cl(2) 92.02(5), Cl(1)-Au(1)-Cl(3) 91.45(5), Cl(2)-Au(1)-Cl(3) 175.22(5), N(1)-C(7)-N(2) 106.4(3).

The Au(III)-$C_{carbene}$ bond length is 1.996(4) Å, slightly shorter than the Au(I)-$C_{carbene}$ bond distances 2.008(5)-2.020(4) Å in **2**, revealing that oxidation of gold(I)-NHC apparently bears no significance for the Au–C bond lengths.[20] Due to the trans effect of the carbene donor, the Au–Cl (1) trans bonds in **4** [2.3062(12) Å] are longer than the Au–Cl (2/3) *cis* bonds [2.2895(12)-2.2826(12) Å]. Like complex **2**, the bond parameters of **4** are very close with other Au(I)-NHC annelated systems developed by our group and mentioned in Table 2. It is concluded from the X-ray structure of **2** and **4** and with comparison of bond parameters of compounds in Table 2 that, the location of the $–CH_3$ group, whether it is in position 'e' or 'i' mentioned in scheme 1 is irrelevant, at least when $N_{pyridine}$ remains uncoordinated. These parameters match the equivalent values observed for related gold(III) monocarbene complexes. [22,23] The N(1)-C(7)-N(2) angle 106.4(3)° is larger than the same angle observed in 2, [N(1)-C(7)-N(2) = 102.8(4)°, N(4)–C(20)–N(5) = 104.3(4) °] and this is due to change in oxidation state from +I to +III.

Biological evaluation

Growth inhibition in cancer cells

The growth inhibitory activities of complexes **2** and **4** were investigated on HepG2, HCT 116, A549 and MCF-7 cells by MTT assay as reported earlier. [24] Treatment of different concentrations of complexes **2** and **4** (0, 2.5, 5, 7.5 and 10 µM) reduced the viability of these cancer cells in a dose dependent manner after 24 h, 48 and 72 h (Fig S1 and S2 with Table 3 and 4). Complex **2** showed relatively higher activity, effecting three fold higher growth inhibition on HepG2 cells with respect to cisplatin and two fold higher growth inhibition than complex **4** (Table 3 and 4). These results are similar to the reports regarding the growth inhibitory effect of other gold-NHC complexes towards a panel of cancer cell lines. [25] However the relatively lower activity of the gold(III)-NHC as compared to gold(I)-NHC complex may be attributed to the reduction of gold (III) → gold (I) upon interaction with intracellular thiols. [4] The NHC ligand **1** failed to elicit any cytotoxicity (Table 5). Unlike cisplatin, none of the gold complexes showed any cytotoxicity towards human Peripheral Blood Mononuclear Cells (PBMCs) (Table 6). As compound **3** is a salt of NHC ligand, $AuCl_2^-$ and $AuCl_4^-$ so its biological activity expected to be negligible, i.e. it is not studied.

Table 3. IC_{50} (µM) of cancer cells in presence of cisplatin and complexes **2** and **4** after 24 h, 48 and 72 h.

Cells	Complex 2 (24 h)	Complex 2 (48 h)	Complex 2 (72 h)
A549	5.12	3.33	1.16
HCT 116	3.91	2.94	1.08
HepG2	3.30	2.66	0.94
MCF-7	4.62	3.47	1.28

Table 4. IC_{50} (µM) of cancer cells in presence of Complexes **4** after 24, 48 and 72 h

Cells	Complex 4 (24 h)	Complex 4 (48 h)	Complex 4 (72 h)
A549	6.19	4.03	2.66
HCT 116	5.78	3.73	2.35
HepG2	6.22	3.91	2.72
MCF-7	5.18	3.29	2.31

Please do not adjust margins

View Article Online
DOI: 10.1039/C5NJ02979A

Published on 05 May 2016. Downloaded by Université Laval on 09/05/2016 06:34:27.

New Journal of Chemistry Accepted Manuscript

Cells were treated with different concentration of proligand, ranging from 0 to 10 µM for 24 h, 48 and 72 h respectively. IC_{50} values were calculated from MTT assay. Values are mean ± S.D and represent one of the 3 representative experiments.

Table 5

IC_{50} (µM) of cancer cells in presence of ligand (**1**.HPF_6) after 24, 48 and 72 h.

Cells	(IC_{50})
HepG2	> 10
HCT-116	> 10
A549	> 10
MCF-7	> 10

Table 6.

IC_{50} of cells in presence of complex **2** and **4** after 24, 48 and 72 h.

Cells	Complex **2** (µM)	Complex **4** (µM)
Peripheral blood mononuclear cells (PBMCs)	> 10	> 10

Cells were treated with different concentration of cisplatin and complex **2** and **4** ranging from 0 to 10 µM for 24 h, 48 and 72 h respectively. IC_{50} values were calculated from MTT assay. Values are mean ± S.D and represent one of the 3 representative experiments.

Induction of apoptosis in HepG2 cells by complex 2

Complex **2** showed higher cytotoxicity towards the HepG2 cell line as compared to the other cancer cell lines used in this study. Therefore the role of complex **2** involved in the induction of apoptosis in HepG2 cells was investigated. Phosphatidylserine [PS] externalization from inner cell membrane to outer membrane is the prerequisite step for apoptosis. Externalized PS can bind with annexin V. [26] After 24 h of treatment with complex 2 (IC_{50} concentration), percentage of apoptotic cells was 58.4 % as compared to 0.1 % in the control cells (Fig. 4). These findings suggest that death of HepG2 cells induced by complex **2** resulted from apoptosis, similar to the earlier reports of induction of apoptosis by Au (I) NHC complexes. [16b]

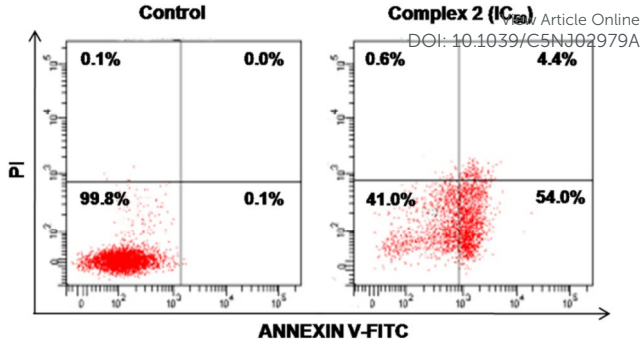

Fig. 4. Flow cytometric analysis of apoptosis induction in HepG2 cells treated with complex **2** (IC_{50} concentration) for 24 h.

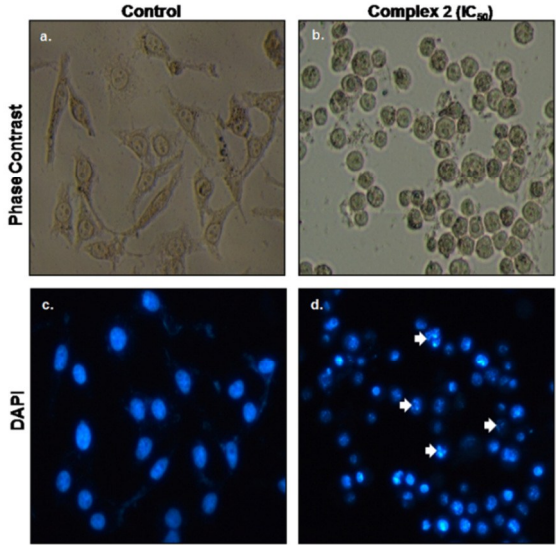

Fig. 5. Morphological images (upper row) of HepG2 cells treated with complex **2** (IC_{50} concentration). DAPI stained image of HepG2 cells (lower row) treated with complex **2** (IC_{50} concentration). Magnification at 20×. Arrows indicate nuclear fragmentation.

Complex **2** induced characteristic apoptotic changes in morphology like cell shrinkage and rounding, chromatin condensation, and DNA fragmentation as revealed by staining with DAPI after 24 h (Fig. 5).

Induction of cell cycle arrest by complex 2

Cell cycle arrest at various phases of cell division precedes apoptosis. [26] Treatment of HepG2 cells with complex **2** (IC_{50} concentration) for 24 h showed a gradual increase in the number of cells in G2/M phase (Figure 6). The percentages of G0/G1 population for the control and complex **2** (IC_{50} concentration) treated HepG2 cells at 24 h were 68.7 % and 58.8 % respectively, indicating a decrease of 9.9 % of cell population in the G0/G1 phase upon complex **2** treatment. The percentages of G2/M population at 24 h were 16.8 % and 26.9 % respectively showing an increase of 10.1 % in cell

This journal is © The Royal Society of Chemistry 20xx

Please do not adjust margins

View Article Online
DOI: 10.1039/C5NJ02279A

population in the G2/M phase and indicating that complex **2** mediates cell cycle arrest at this phase in HepG2 cells (Fig. 6).

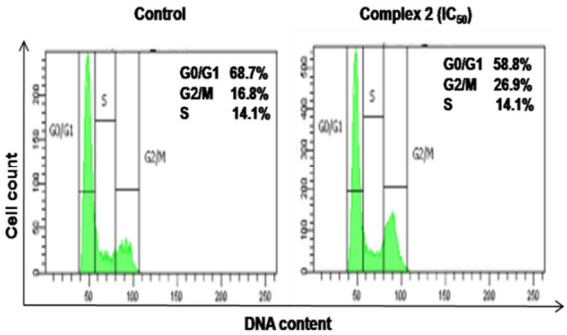

Fig. 6. Cell cycle analysis of complex **2** (IC_{50} concentration) treated HepG2 cells for 24 h.

Role of complex 2 in ROS generation and mitochondrial membrane potential

Generation of intracellular ROS has been considered as a key factor in apoptosis. Therefore the role of ROS generation in complex **2** induced apoptosis was evaluated. Treatment of HepG2 cells with the complex (IC_{50} concentration) for 24 h led to change in DCF mean intensity from 567 to 12,659, indicating a shift in ROS generation from the control cells to complex **2** (IC_{50} concentration) treated cells (Fig. 7a). Moreover, treatment of HepG2 cells with complex **2** (IC_{50} concentration) for 24 h led to a loss in mitochondrial membrane potential (ΔΨm) with 62.6 % cells showing loss of ΔΨm following treatment with complex **2** as compared to 4.3 % of the control cells (Fig. 7b). Our results were similar to other reports on generation of ROS and loss of ΔΨm following treatment of cancer cells with Au(I)-NHC complexes. [24]

Complex 2 mediated apoptosis of HepG2 cells proceeds via the mitochondrial death pathway

The efficacy of complex **2** was also evaluated on the expression of mitochondrial proteins in HepG2 cells. Treatment of HepG2 cells with complex **2** for 24 h altered the Bax/Bcl-2 ratio, increased cytosolic cytochrome c, and decreased pro-caspase 9 and 3 expression levels, leading to PARP cleavage (Fig. 8). Therefore complex **2** mediated cell death may proceed via the mitochondrial death pathway.

Role of complex 2 in p53 and p21 expression

HepG2 cells possess wild type p53 which generally has a role to play in apoptosis. Thereby, the role of p53 in complex **2** mediated apoptosis was evaluated. Cells were treated with complex **2** (IC_{50} concentration) for 24 h and immuno-fluorescence studies were conducted, which revealed increased expressions of p53 and p21 along with nuclear translocation of p53 (Fig. 9). Similar high expressions of p53 and p21 by treatment of gold (I) NHC complexes were also reported on other cancer cancer cell lines. [25] Therefore complex **2** mediated cell death may involve p53 as a possible mediator of apoptosis.

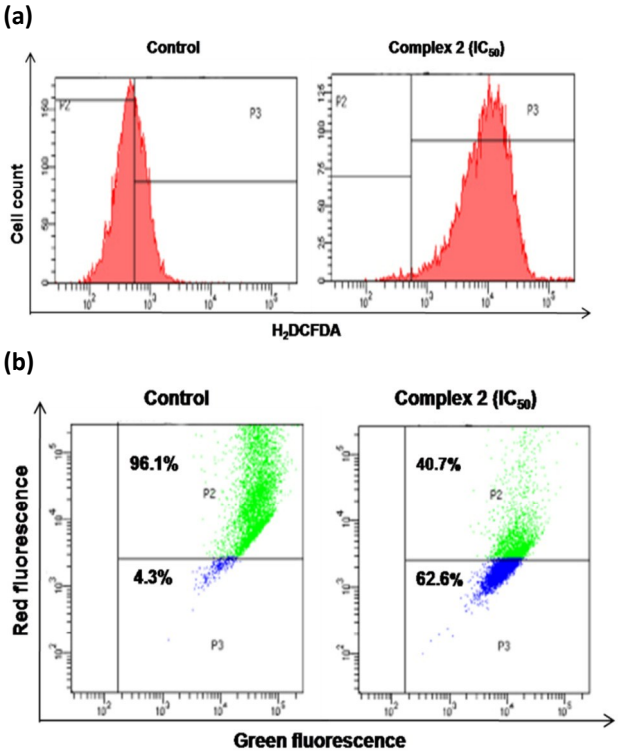

Fig. 7. (a) Flow cytometric analysis of ROS generation in cells 24 h after treatment with complex **2** (IC_{50} concentration). (b) Flowcytometric analysis of loss of ΔΨm in presence of complex **2** (IC_{50} concentration) after 24 h.

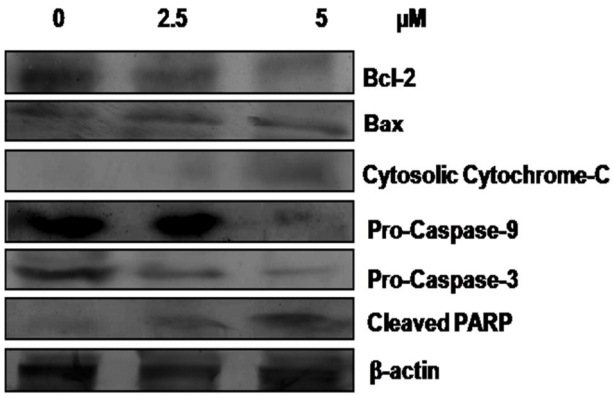

Fig. 8. Expression of various pro and anti apoptotic proteins following treatment of HepG2 cells with complex **2** (0, 2.5 and 5 μM) for 24 h, with β-actin as loading control.

Published on 05 May 2016. Downloaded by Université Laval on 09/05/2016 06:34:27.

New Journal of Chemistry Accepted Manuscript

Please do not adjust margins

View Article Online
DOI: 10.1039/C5NJ02979A

ARTICLE

Published on 05 May 2016. Downloaded by Université Laval on 09/05/2016 06:34:27.

New Journal of Chemistry Accepted Manuscript

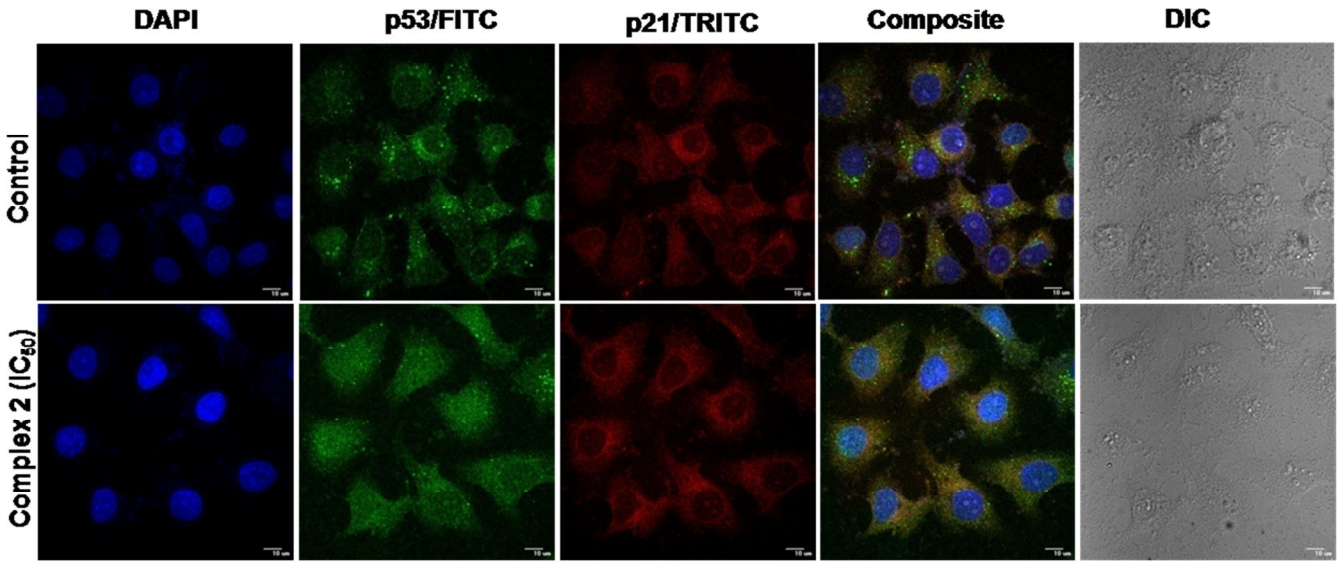

Fig. 9. Upregulation of p53, p21 and subsequent nuclear translocation of p53 upon treatment of cells with complex 2 (IC_{50} concentration). Scale Bar = 15 mm. Magnification at 40 ×.

Conclusion

We have synthesized and spectroscopically characterized Au(I) and Au(III)-NHC complexes **2, 3** and **4** and determined their solid state structures by single crystal X – ray diffraction studies. Gold(III)-NHC complex (**4**) has been synthesized by disproportionation pathway from the gold(I)-NHC complex (**2**) and the isolated intermediate confirmed the disproportionation pathway where both Au (I) and Au (III) are present. Exploration of the cytotoxic effects of the Au(I) and Au(III) complexes was performed on a panel of cancer cells, namely, HepG2, HCT 116 and it is found Au(I)-NHC, **2** is more potent than Au(III)-NHC, **4**.

Experimental Section

General procedures

The reagents Ag_2O, NH_4PF_6, pyridine-2-carboxaldehyde, and 2-amino-6-methylpyridine were purchased from Sigma Aldrich, UK and used without further purification. $Au(SMe_2)Cl$ was prepared by the reported procedure. [27] All manipulations were carried out under open atmosphere. All solvents were distilled over appropriate drying agents and N_2-saturated prior to use. NMR spectra were measured on Bruker 300 and 100.5 spectrometers at 25°C with tetramethylsilane as an internal standard. Electronic spectra of the complexes were obtained on a Shimadzu UV-1601 spectrophotometer.

General syntheses

Synthesis of 1·HPF$_6$: Proligand **1**·HPF_6 was prepared by the reported procedure [16] with slight modification which improved the yield. 2-Pyridyl-*N*-2-(6-methylpyridine)methylamine (2 g, 10.9 mmol), 2 drops formic acid, 0.5 ml triethyl orthoformate and crushed 91% paraformaldehyde powder (0.360 g, 10.9 mmol) were taken in 20 ml dioxane and refluxed for 8 h; rest of the procedure was as reported earlier. Yield was 2.79 g (7.86 mM, 79%).

Preparation of [Au(1)$_2$] [PF$_6$] (2) : The proligand **1**·HPF_6 (250 mg, 0.70 mmol) and silver oxide (0.085 g, 0.037 mmol) were taken in dry acetonitrile and stirred at room temperature for 4 h. The solution was filtered through a plug of celite to remove the unreacted Ag_2O; the solvent was removed and the solid was dried in vacuum. Acetonitrile solution of

Please do not adjust margins

Please do not adjust margins

View Article Online
DOI: 10.1039/C5NJ02979A

Published on 05 May 2016. Downloaded by Université Laval on 09/05/2016 06:34:27.

New Journal of Chemistry Accepted Manuscript

$Au(SMe_2)Cl$ was added dropwise to the prepared silver complex, when immediate white ppt was observed. The silver halide AgCl was removed through filtration, the solvent was stripped off, and the solid was dried over silica. The compound was recrystallised from CH_3CN/Et_2O. Yield was 87% (266 mg, 0.35 mmol). ^{1}H NMR (DMSO-d_6, 300 MHz, 25 °C) δ 8.65 (d, J = 3.0 Hz, 1H, H^a), 8.54 (s, 1H, H^e), 8.04 (d, J = 7.0 Hz, 1H, 1H, H^d), 7.90 (t, J = 7.2 Hz, 1H, H^c), 7.72 (d, J = 9.0 Hz, 1H, H^f), 7.61 (d, J = 9.0 Hz, 1H, H^h), 7.00 (m, 1H, H^b), 6.87 (m, 1H, H^g), 2.62 (s, 3H, -CH_3). ^{13}C NMR (DMSO-d_6, 100.5 MHz, 25 °C) δ: 171.9, 158.5, 151.8, 137.3, 137.1, 127.1, 126.4, 123.5, 122.1, 120.6, 117.8, 117.0, 11.8. Anal. Calc. for $AuC_{26}H_{22}N_6PF_6$: C, 41.05; H, 2.89; N, 11.05%. Found: C, 40.63; H, 2.83; N, 10.92%.

Preparation of $[1/2AuCl_2, 1/2AuCl_4]^-$ $[(1H)]^+$ (3) : Complex **2** (200 mg, 0.27 mmol) was dissolved in acetonitrile (10 ml) at room temperature; $Au(SMe_2)Cl$ (230 mg, 0.78 mmol) was added to the solution and stirring continued for 4 h. The colour of the solution changed from colorless to light yellow. Then solvent acetonitrile was removed and the yellow complex was recrystallized from acetonitrile and diethyl ether. Yield was 78% (132 mg, 0.20 mmol). ^{1}H NMR (DMSO-d_6, 300 MHz, 25 °C) δ 11.05 (s, 1H, H^j), 8.91 (s,1H, H^e), 8.39 (d, J = 3.0 Hz, 1H, H^a), 8.32 (m, 2H, $H^{b,c}$), 8.15 (t, J = 7.8 Hz, 1H, H^g), 7.90 (d, J = 7.0 Hz, 2H, $H^{d,f}$), 7.40 (d, J = 7.5 Hz, 1H, H^h), 2.54 (s, 3H, –CH_3).^{13}C NMR (DMSO-d_6, 100.5 MHz): 149.0, 146.1, 140.1, 129.2, 125.2, 124.7, 124.1, 123.5, 117.9, 114.2, 109.4, 108.9, 11.2. Anal. Calc. for $C_{13}H_{12}N_3$,0.5(Au_2Cl_6): C, 23.69; H, 1.82; N, 6.38 %. Found: C, 23.63; H, 1.79; N, 6.36 %.

Preparation and $[Au(1)Cl_3]$ (4) : Complex **3** (200 mg, 0.27 mmol) was dissolved in acetonitrile (10 ml) at room temperature; $Au(SMe_2)Cl$ (160 mg, 0.54 mmol) was added to the solution and stirring continued for 5-6 h. The colour of the solution changed from colourless to yellow with a slight precipitate. The precipitate of metallic gold was reused to synthesize $Au(SMe_2)Cl$. After filtration the acetonitrile was removed under vacuum and at low temperature to obtain a yellow powder. The yellow complex was recrystallized from acetonitrile and diethyl ether. Yield was 68% (91 mg, 0.17 mmol). ^{1}H NMR (DMSO-d_6, 300 MHz, 25 °C) δ 9.08 (s,1H, H^e), 8.81 (d, J = 7.1 Hz, 1H, H^a), 8.17 (d, J = 7.2, 1H, H^d), 8.05 (t, J = 7.1, 1H, H^c), 7.72 (d, J = 7.5 Hz, 1H, H^f), 7.61 (d, J = 7.3, 1H, H^h), 7.32 (m, 1H, H^b), 7.21 (t, 1H, H^g), 2.73 (s, 3H, –CH_3). ^{13}C NMR (DMSO-d_6, 100.5 MHz, 25 °C) δ: 159.3, 146.4, 141.1, 130.6, 126.0, 125.9, 125.5, 124.9, 119.4, 119.1, 112.4, 110.4, 12.2. Anal. Calc. for $AuC_{13}H_{11}N_3Cl_3$: C, 30.49; H, 2.14; N, 8.19%. Found: C, 30.41; H, 2.09; N, 8.11%.

Crystal structure determinations

Single crystals of **2**, **3** and **4** suitable for X-ray data collection were grown by slow diffusion of diethyl ether into a saturated acetonitrile solution of the respective complexes. The crystal data and details of the data collected for **2, 3** and **4** are given in Table 1. X-ray data were collected on a CCD diffractometer (graphite monochromated Mo Ka radiation, k = 0.71073A˚). The structures were solved by direct methods and refined on F2 using all reflections with SHELX-97.[28] The nonhydrogen atoms were refined anisotropically. Hydrogen atoms which were not bound to imidazolium-C2 atoms were placed in calculated positions and assigned to an isotropic displacement parameter of 0.08 Å.

Cell culture

Cell lines such as HepG2 (human hepatocellular carcinoma), HCT 116 (human colorectal carcinoma), A549 (human non small lung carcinoma) and MCF-7 (human breast adenocarcinoma) were obtained from National Centre for Cell Science, Pune, India. The cell lines were cultured in DMEM supplemented with 10% FBS and 1% antibiotic (PSN) and incubated at 37 °C in a humidified atmosphere with 5% CO_2. After achieving 75–80% confluence, cells were harvested with 0.025% trypsin and 0.52 mM EDTA in phosphate buffered saline (PBS) and seeded at desired density to allow them to re-equilibrate a day before the start of experimentation. All experiments were conducted in DMEM supplemented with 10% FBS and 1% antibiotic (PSN) solution.

Cell viability assay

Cells (5000 cells per well) were treated with various concentrations of complexes **2, 3** and **4** (0, 2.5, 5, 7.5 and 10 µM) for 24, 48 and 72 h (dissolved in DMSO) and their respective IC_{50} values were determined by MTT assay as described earlier.[29] Absorbance of the solubilized intracellular formazan was measured at 595 nm using an ELISA reader (Model: Emax, Molecular Device, USA).

Detection of apoptosis using flow cytometry

Apoptosis was assayed by using an annexin V-FITC apoptosis detection kit (Calbiochem, La Jolla, CA) as described earlier. [26] HepG2 (1 X 10^6) cells treated with complex **2** (IC_{50} concentration) for 24 h were stained with PI and annexin V-

Please do not adjust margins

View Article Online
DOI: 10.1039/C5NJ02979A

FITC according to manufacturer's instructions. The percentage of live, apoptotic and necrotic cells were analyzed by BD LSRFortessa cell analyzer (Becton Dickinson, San Jose, CA, USA). Data from 10^4 cells were analyzed for each sample.

Assessment of cellular death parameters

HepG2 (1 X 10^4) cells treated with complex **2** (IC_{50} concentration) for 24 h were viewed under a phase contrast microscope. Cells were stained with DAPI (4', 6-diamidino-2-phenylindole) for the detection of chromatin condensation and DNA fragmentations and observed under an inverted phase contrast/fluorescent microscope (Model: OLYMPUS IX70, Olympus Optical Co. Ltd., Shibuya-ku, Tokyo, Japan), and images were acquired as described earlier. [29]

Analysis of cell cycle arrest

Cell cycle arrest was analyzed by treating HepG2 (1 X 10^6) cells with complex **2** (IC_{50} concentration) for 24 h followed by PI staining, as described earlier.[25] The percentages of cell population undergoing cell cycle arrest at various stages of cell division were analyzed by BD LSRFortessa cell analyzer (Becton Dickinson, San Jose, CA, USA). Data from 10^4 cells were analyzed for each sample.

Measurement of intra cellular ROS level upon treatment of HepG2 cells with complex 2

For the detection of intracellular ROS generation, HepG2 (1 X 10^6) cells treated with complex **2** (IC_{50} concentration) for 24 h were incubated with 10 µM of H2DCFH-DA (2',7',-dichlorofluorescein diacetate, Molecular Probes) for 25 min at 37 °C, following which cells were analyzed by BD LSRFortessa cell analyzer. Data from 10^4 cells were analyzed for each sample as described earlier. [30]

Measurement of mitochondrial membrane potential

To measure the mitochondrial membrane potential (Δψm), HepG2 cells treated with complex **2** (IC_{50} concentration) for 24 h were incubated with JC-1 (5,5´,6,6´-tetrachloro-1,1´,3,3´-tetraethylbenzimidazolyl carbo-cyanine iodide, Sigma) which gives fluorescence in the FITC channel for green monomers in case of healthy cells having high mitochondrial membrane potential and in the PE-Texas Red A channel for red aggregates indicating a drop in the mitochondrial membrane potential signifying apoptotic cells (BD LSRFortessa cell analyzer). Data from 10^4 cells were analyzed for each sample. [31]

Confocal microscopy for immunocytochemistry studies

HepG2 cells were treated with complex **2** (IC_{50} concentration) for 24 h and confocal microscopy for immunocytochemical analysis of the expressions of p53 and p21 was done as reported earlier. [30] Cells were observed under an Andor spinning disk confocal microscope and images were acquired.

Western blot analysis of protein expression in HepG2 cells following treatment with complex 2

Western blotting of the lysates of the cells treated with complex **2** (0, 5 and 7.5 µM) for 24 h was performed on 10-15 % SDS-PAGE gels, using primary antibodies, alkaline phosphatase conjugated secondary antibodies and NBT-BCIP as a chromogenic substrate as described earlier. [32] Western blots were done for the detection of PARP cleavage, and expression levels of pro-caspase 3 and pro-caspase 9, along with cytosolic cytochrome c, Bax and Bcl-2.

Statistical analysis

All the experiments were carried out in triplicate and values were reported as mean ± SD. Student's t test was used for determining statistical significance (*P<0.05 and **P<0.01).

MCF-7 and A549. Au(I) complex **2** showed higher cytotoxicity towards HepG2 cell line than the Au(III)-NHC complex. Production of ROS and loss of Δψm and caspase 9 and caspase 3 activities indicated that complex **2** induces apoptosis in HepG2 cells through mitochondrial death pathway with increased expressions of p53 and p21. This may prove useful in formulation of lead compounds against hepatocellular carcinoma that harbour wild type p53.

Associated content

# Both **Tapastaru Samanta** and **Abhishek Nandy** contributed equally to this work**.**

Acknowledgements

J.D. is grateful to DST, India, for financial support under 'Young Scientist Scheme' (SR/FT/CS-046/2009). J.D. is also grateful to hon'ble Vice Chancellor Prof. A. K. Das and hon'ble Chairman PG Council Prof. R. K. Bal for constant encouragement. We are thankful Mr. Diptadeep Sarkar and Ms Anushila Gangopadhyay for microscope and Flow Cytometer facility. S. A. extends sincere appreciation to the deanship of scientific research at King Saud University for its funding through Prolific Research group PRG-1436 – 03.

Published on 05 May 2016. Downloaded by Université Laval on 09/05/2016 06:34:27.

New Journal of Chemistry Accepted Manuscript

This journal is © The Royal Society of Chemistry 20xx

Please do not adjust margins

View Article Online
DOI: 10.1039/C5NJ02979A

Keywords: N-Heterocyclic Carbene • Gold(I)-NHC • Gold(III)-NHC • Disproportion • Cytotoxicity

Supporting information

Crystallographic data for complexes **2**, **3** and **4** in CIF format; are available free of charge via the Internet at under http://dx.doi.org/xxxxxxx/ejic.xxxxxx.

Notes and references

[a] *Cancer Biology and Inflammatory Disorder Division, Indian Institute of Chemical Biology, Kolkata-700032, India*

[b] *School of Applied Science, Haldia Institute of Technology, Haldia-721657, Purba Medinipur, West Bengal, India*

[c] *Department of Inorganic Chemistry, Indian Association for the Cultivation of Sciences, Jadavpur, Kolkata-700032, West Bengal, India*

[d] *Department of Physics, Jadavpur University, Jadavpur, Kolkata-700032, West Bengal, India*

[e] *Chemistry Department, College of Science, King Saud University, B.O. Box 2455, Riyadh, 11451, Saudi Arabia*

[f] *Department of Chemistry, Utkal University, Bhubaneswar-751004, Odisha., India.*

Corresponding Authors

Prof. Joydev Dinda

e.mail: joydevdinda@gmail.com , dindajoy@yahoo.com

References

1 M. Frezza, S. Hindo, D. Chen, A. Davenport, S. Schmitt, D. Tomco, Q. P. Dou, *Curr. Pharm. Des*, 2010, 16, 1813-1825.

2 B. Rosenberg, L.Vancamp, J. E. Trosko, V. H. Mansour, *Nature*. 1969, **222**, 385-386.

3 G. Gasser, I. Ott, N. M. Nolte, *J. Med. Chem*. 2011, **54**, 3–25.

4 T. Zou, C. T. Lum, S. S. Y. Chui, C. M. Che, *Angew. Chem. Inter. Ed.* 2013, **52**, 2930-2933.

5 R. W. Y. Sun, D.L. Ma, E.L.M. Wong, C.M. Che, *Dalton Trans*. 2007, 4884-4892.

6 M. L. Teyssot, A. S. Jarrousse, M. Manin, A. Chevry, S. Roche, F. Norre,; C. Beaudoin,; L. Morel, D. Boyer, R. Mahiou, A. Gautier, *Dalton Trans*. 2009, 6894–6902.

7 S. Patil, J. Claffey, A. Deally, M. Hogan, B. Gleeson, L. M. M. Méndez, H. M. Bunz, F. Paradisi, M. Tacke, *Eur. J. Inorg. Chem*. 2010, 1020-1031.

8 a) J. R. Miecznikowski, S. Gruendemann, M. Albrecht, C. Megret, E. Clot, J. W. Faller, O. Eisenstein, R. H. Crabtree, *Dalton Trans*. 2003, 831-838; b) C. M. Crudden, D. P. Allen, *Coord. Chem. Rev*. 2004, **248**, 2247-2273; c) A. G. Tennyson, V. M. Lynch, C. W. Bielawski, *J. Am. Chem. Soc*. 2010, **132**, 9420-9429.

9 B. Cetinkaya, E. Cetinkaya, H. Kucubay, R. Durmaz Arzneim. *Forsch, Drug. Res*. 1996, **46**, 821-823.

10 a) S. Gaillard, A. M. Z. Slawin, A. T. Bonura, E. D. Stevens, S. P. Nolan, *Organometallics*. 2010, **29**, 394-402; b) W. Liu, K. Bensdorf, M. Proetto, U. Abram, A. Hagenbach, R. Gust, *J. Med. Chem*. 2011, 54, 8605-8615; c) C.Topf, C. Hirtenlehner, M. Zabel, M. List, M. Fleck, Monkowius, U. *Organometallics*. 2011, **30**, 2755–2764; d) J. Dinda, S. D. Adhikary, S. K. Seth, A. Mahapatra, *New J. Chem*. 2013, **37**, 431-438.

11 a) W. Liu, R. Gust, *Chem. Soc. Rev*. 2013, **42**, 755-773; b) F. Cisnetti, A. Gautier, *Angew. Chem. Int. Ed*. 2013, **52**, 11976-11978; c) L. Oehninger, R. Rubbiani, I. Ott, *Dalton Trans*. 2013, **42**, 3269-3284. (d) A. Gautier, F. Cisnetti, *Metallomics*. 2012, **4**, 23–32.

1 a) W. Liu, K. Bensdorf, M. Proetto, U. Abram, A. Hagenbach, R. Gust, *J. Med. Chem*. 2011, **54**, 8605-8615; b) E. Schuh, C. Pflüger, A. Citta, A. Folda, M. P. Rigobello, A. Bindoli, A. Casini, F. Mohr, *J. Med. Chem*. 2012, **55**, 5518-5528.

13 P. J. Barnard, S. Berners-Price, *J. Coord. Chem. Rev*. 2007, 2519, 1889–1902.

Published on 05 May 2016. Downloaded by Université Laval on 09/05/2016 06:34:27.

New Journal of Chemistry Accepted Manuscript

Please do not adjust margins

View Article Online
DOI: 10.1039/C5NJ02979A

14 J. L. Hickey, R. A. Ruhayel, P. J. Barnerd, M. V. Baker, S. J. Berners-Price, A. Filipovska, *J. Am. Chem. Soc.* 2008, **30**, 12570–12571.

15 V. Milacic, Q.P. Dou, *Coord Chem Rev.* 2009, **253**, 1649-1660.

16 a) S. D. Adhikary, D. Bose, P. Mitra, K. D. Saha, V. Bertolasi, J. Dinda, *New J. Chem*. 2012, **36**, 759-767; b) A.Nandy, S. K.Dey, S. Das, R. N.Munda, J. Dinda, K. D. Saha, *Molecular Cancer*. 2014, **13**, 1-14.

17 a) D. Fan, C. T. Yang, J. D. Ranford, P. F. Lee, J. J. Vittal, *J. Chem. Soc. Dalton Trans*. 2003, 2680-2685; b) D. Fan, C.-T.ong Yang, J. D.Ranford, J. J. Vittal, P. F. Lee, *Dalton Trans*. 2003, 3376–3381.

18 R. Cao, J. Jia, X. Ma, M. Zhou, H. Fei, *J. Med. Chem*. 2013, **56**, 3636−3644.

19 T. Samanta, B. K.Rana, G. Roymahapatra, S. Giri, P. Mitra, R. Pallepogu, P. K. Chattaraj, J. Dinda, *Inorg. Chim. Acta*. 2011, **375**, 271-279.

20 H. M. J. Wang, I. J. B. Lin, *Organometallics*. 1998, **17**, 972-975.

21 a) J. Dinda, T. Samanta, A. Nandy, K. D.Saha, S. K.Seth, S. K. Chattopadhyay, C. W. Bielawski, *New J. Chem*. 2014**,** **38,** 1218-1224; b) B**.** Rana, A. Nandy, V.Bertolasi, C.W. Bielawski, K. D. Saha, J. Dinda, *Organometallics*. 2014, **33**, 2544−2548.

22 a) S. Gaillard, M. Z. Slawin, A. T. Bonura, E. D. Ste-vens, S. P. Nolan, *Organometallics*. 2010, **29**, 394-402; b) P. Fre´mont, R. Singh, E. D. Stevens, J. L. Peterson, S. P. Nolan, *Organometallics*. 2007, **26**, 1376-1385.

23 a) T. Samanta, L. R. Dey, J. Dinda, S. K. Chat-topadhyay, S. K. Seth, *J. Mol. Structure*. 2014, **1068**, 58-70; b) J. Boydston, J. D. Rice, M. D. Sanderson, O. L. Dykhno, C. W. Bielawski, *Organometallics*. 2006, **25**, 6087-6098 and ref. therein.

24 R. Rubbiani, I. Kitanovic, H. Alborzinia, S. Can, A. Kitanovic, L. A. Onambele, M. Stefanopoulou, Y. Geldmacher, W. S. Sheldrick, G. Wolber, A. Prokop, S. Wölfl, I. Ott, *J. Med. Chem*. 2010, **53**, 8608-8618.

25 C. H. Wang, W. C. Shih, H. C. Chang, Y. Y. Kuo, W. C. Hung, T. G. Ong, W. S. Li, *J Med Chem*. 2011, **54**, 5245-5249.

26 S. Mallick, B. C. Pal, J. R.Vedasiromoni, D. Kumar, K. D. Saha, *Cell. Physiol Biochem*. 2012, **30**, 915-926.

27 R. Uson,; A. Laguna, M. Laguna, *Inorg. Synth*. 1989, **26**, 85-91.

28 G. M. Sheldrick, SHELX-97, Program for Crystal Structure Refinement, University of Gottingen, Germany (1997).

29 T. J. Mosmann, *Immunol. Methods*. 1983, **65**, 55-63.

30 S. K. Dey, D. Bose, A. Hazra, S. Naskar, A. Nandy, R. N. Munda, S. Das, N. Chatterjee, N. B. Mondal, S. Banerjee, K. D. Saha, *PLoS One*. 2013, **8**, e58055.

31 S. Mallick, B. C. Pal, D. Kumar, N.Chatterjee, S.Das, K. D. Saha, *J. Asian Nat. Prod. Res*. 2013, **15**, 1197-1203.

32 S. Das, N. Chatterjee, D. Bose, S. K. Dey, R. N. Munda, A. Nandy, S. Bera, S. K. Biswas, K. D. Saha, *Cell. Physiol. Biochem*. 2012, **29**, 251-260.

Published on 05 May 2016. Downloaded by Université Laval on 09/05/2016 06:34:27.

New Journal of Chemistry Accepted Manuscript

This journal is © The Royal Society of Chemistry 20xx

Please do not adjust margins

View Article Online
DOI: 10.1039/C5NJ02979A

Synthesis of Gold(III)←Gold(I)-NHC Through Disproportionation: Role of Gold(I)-NHC in the induction of apoptosis in HepG2 cells

Abhishek Nandy [a], Tapastaru Samanta,[b] Sumana Mallick, [a] Partha Mitra,[c] Saikat Kumar Seth, [d] Krishna Das Saha[a]*, Salem S. Al-Deyab [e] and Joydev Dinda[f]*

[a] *Cancer Biology and Inflammatory Disorder Division, CSIR-Indian Institute of Chemical Biology, Kolkata-700032, India*

[b] *School of Applied Science, "Applied Synthetic Chemical Research Laboratory", Haldia Institute of Technology, Haldia-721657, Purba Medinipur, West Bengal, India*

[c] *Department of Inorganic Chemistry, Indian Association for the Cultivation of Sciences, Jadavpur, Kolkata-700032, West Bengal, India*

[d] *Department of Physics, Jadavpur University , Jadavpur, Kolkata-700032, West Bengal, India*

[e] *Chemistry Department, College of Science, King Saud University, B.O. Box 2455, Riyadh, 11451, Saudi Arabia*

[f] *Department of Chemistry, ITM University-Gwalior, Gwalior-474001, M.P., India.*

Published on 05 May 2016. Downloaded by Université Laval on 09/05/2016 06:34:27.

Anticancer activities of the novel Au(I) and Au(III)-NHC complexes have been performed based on 2-[(6-methylpyridin-2-yl)]imidazo[1,5-a]pyridin-4-ylium hexafluorophosphate.

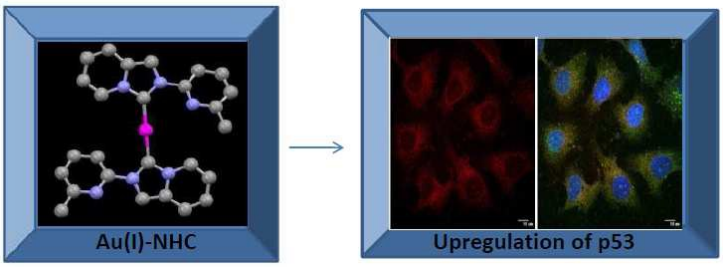

New Journal of Chemistry Accepted Manuscript